International Journal of Biological Macromolecules 273 (2024) 133215

Contents lists available at ScienceDirect

International Journal of Biological Macromolecules

journal homepage: www.elsevier.com/locate/ijbiomac

# *Limosilactobacillus fermentum* strains MC1 and D12: Functional properties and exopolysaccharides characterization

Nina Čuljak [a], Barbara Bellich [b,1], Alice Pedroni [c,2], Katarina Butorac [a], Andreja Leboš Pavunc [a], Jasna Novak [a], Martina Banić [a], Jagoda Šušković [a], Paola Cescutti [c,*], Blaženka Kos [a]

[a] Laboratory for Antibiotic, Enzyme, Probiotic and Starter Cultures Technology, Department of Biochemical Engineering, University of Zagreb Faculty of Food Technology and Biotechnology, Pierottijeva 6, 10000 Zagreb, Croatia
[b] Department of Advanced Translational Diagnostics, Institute for Maternal and Child Health, IRCCS "Burlo Garofolo", Via dell'Istria 65, 34137 Trieste, Italy
[c] Department of Life Sciences, University of Trieste, Via Licio Giorgieri 1, Bdg. C11, 34127 Trieste, Italy

ARTICLE INFO

*Keywords:*
Exopolysaccharides structure
*Limosilactobacillus fermentum*
NMR
Whole-genome sequencing
Probiotic

ABSTRACT

Lactic acid bacteria (LAB) produce a broad spectrum of exopolysaccharides (EPSs), commonly used as texturizers in food products. Due to their potential contribution to LAB probiotic properties, like adhesion to human epithelial cells and competitive exclusion of pathogens from human intestinal epithelial cells, this study was focussed on the structural and functional characterization of the EPSs produced by two *Limosilactobacillus fermentum* strains – MC1, originating from mother's milk, and D12, autochthonous from Croatian smoked fresh cheese. Whole-genome sequencing and functional annotation of both L. *fermentum* strains by RAST server revealed the genes involved in EPS production and transport, with some differences in functionally related genes. EPSs were extracted from the cell surface of both bacterial strains and purified by size-exclusion chromatography. Structural characterization of the EPSs, achieved by chemical analyses and 1D and 2D NMR spectroscopy, showed that both strains produce an identical mixture of three different EPSs containing galactofuranose and glucopyranose residues. However, a comparison of the functional properties showed that the MC1 strain adhered better to the Caco-2 cell line and exhibited stronger antimicrobial effect against *Salmonella enterica* serovar Typhimurium FP1 than the D12 strain, which may be attributed to the potential bacteriocin activity of the MC1 strain.

## 1. Introduction

Exopolysaccharides (EPSs) are extracellular macromolecules produced by microorganisms in the form of a strongly bound capsule or a loose mucus layer [1]. In addition to improving the organoleptic properties and extending the shelf life of fermented foods [2], EPSs can also have antimicrobial, anti-inflammatory, antitumor, antiviral, antioxidant, immunomodulatory, antidiabetic, antiulcer and cholesterol-lowering effects [3,4]. Different bacteria, fungi and certain algae have the ability to produce EPSs [5]. EPSs produced by lactic acid bacteria (LAB) were selected for numerous applications due to their "generally regarded as safe" (GRAS) status and their potential use as probiotics [6]. EPS production is strain-specific and EPSs are usually produced in small quantities. Deo et al. [7] point to major differences in the composition and organization of genes involved in EPSs biosynthesis in *Lactobacillus* strains. Despite their great structural diversity, EPSs can be assembled by microorganisms through four common pathways: (1) the extracellular synthesis pathway, (2) the ATP-binding cassette (ABC) transporter-dependent pathway, (3) the synthase-dependent pathway and (4) the Wzx/Wzy-dependent pathway [8]. The most distinguished EPS-producing LAB are *Limosilactobacillus, Lacticaseibacillus, Lactiplantibacillus, Lactobacillus, Lactococcus, Latilactobacillus, Lentilactobacillus, Leuconostoc, Pediococcus, Streptococcus, Fructilactobacillus* and *Weissella* species, which are capable of synthesizing a variety of EPSs [9,10]. EPSs might be of central importance in enhancing the probiotic properties of LAB strains, *e.g.* through protecting bacterial cells from stressful

* Corresponding author.
*E-mail address:* pcescutti@units.it (P. Cescutti).
[1] When the experiments were performed Barbara Bellich was working at Department of Life Sciences, University of Trieste, *Via* Licio Giorgieri 1, Bdg. C11, 34,127 Trieste, Italy.
[2] Present address: Delft University of Technology, Department of Biotechnology, van der Maasweg 9, Delft, 2629HZ, The Netherlands.

https://doi.org/10.1016/j.ijbiomac.2024.133215
Received 29 March 2024; Received in revised form 17 May 2024; Accepted 15 June 2024
Available online 17 June 2024

environmental conditions or adverse compounds [11,12]. They are associated with biofilm formation [13] and host-pathogen interactions [14], and may play a major role in adhesion to eukaryotic cells and in modulating the host immune system [15,16].

LAB are omnipresent, including dairy and non-dairy based products or can be isolated from animal origin like meat and meat products [9]. Another source of probiotic bacteria is mother's milk [17,18], which contains nutrients such as proteins, lipids, carbohydrates, vitamins and minerals and is the optimal food for neonates [19]. The growth and metabolism of microorganisms varies depending on the source and environmental conditions, and it has been shown that the yield of EPSs depends on the producing strain as well as cultivation and environmental conditions [20]. The EPSs produced by LAB strains differ in their chemical composition and structure, which directly affects the protective role of the producing cells under unfavorable environmental conditions, adhesion properties and interaction with specific receptors of the host defense system, which have been scarcely described in EPSs derived from LAB [21].

It has been disclosed that some *Limosilactobacillus fermentum* strains are capable of producing EPSs, but their contribution to the functional properties of the producing strains remains to be investigated. This paper describes the characterization of the EPSs produced as well as adhesion and antimicrobial properties of *Limosilactobacillus fermentum* MC1 strain, isolated from human milk [17], and *Limosilactobacillus fermentum* D12 strain, previously isolated and characterized by our group from smoked fresh cheese from the Zagorje region (Croatia) [11].

## 2. Materials and methods

### 2.1. Bacterial strains and cell line

The EPS-producing *Limosilactobacillus fermentum* MC1 and *Limosilactobacillus fermentum* D12, isolated from mother's milk and smoked fresh cheese, respectively, were stored as frozen stocks at −80 °C in de Man Rogosa Sharpe (MRS) broth (BD Difco, USA) supplemented with 15 % *v*/v glycerol, while *Escherichia coli* 3014 and *Salmonella enterica* serovar Typhimurium FP1 were maintained in nutrient broth (Biolife, Italy) supplemented with 15 % v/v glycerol. All strains used in this study are part of the Culture collection of the Laboratory for Antibiotic, Enzyme, Probiotic and Starter Cultures Technology, University of Zagreb Faculty of Food Technology and Biotechnology. Prior to each experiment, strains L. *fermentum* MC1 and D12 were grown in MRS broth (BD Difco, USA) medium overnight at 37 °C under anaerobic conditions, while *E. coli* 3014 and *S.* Typhimurium FP1 were grown overnight at 37 °C in nutrient broth (Biolife, Italy) under aerobic conditions.

The Caco-2 cell line, which contains heterogeneous human tumor cells of the colorectal epithelium, was used in this work to study LAB adhesion and competitive exclusion of potentially pathogenic bacteria. Caco-2 cells are stored in EMEM medium (Eagle's minimal essential medium; Thermo Fisher Scientific, USA) at -−80 °C with the addition of 10 % glycerol. The Caco-2 cell line used in the experiments is part of the collection of the Laboratory for Biology and Microbial Genetics of the University of Zagreb Faculty of Food Technology and Biotechnology (American Type Culture Collection, ATCC HTB-37, USA). Research activities were performed in compliance with all regulatory requirements and quality and safety standards.

### 2.2. Whole-genome sequencing (WGS) and detection of genes responsible for exopolysaccharides (EPSs) production

The L. *fermentum* MC1 genomic DNA was isolated according to Butorac et al. [11], and sequenced on the Illumina MiSeq 2500 (Illumina, USA) at IGA Technology Services (Italy) using a method described in Banić et al. [22]. The L. *fermentum* MC1 genome was analyzed using the RAST server (Rapid Annotations using Subsystems Technology; http://rast.nmpdr.org/rast.cgi), which performs annotation of prokaryotic genomes by identifying protein-coding, rRNA and tRNA genes, assigning them a function, predicting which subsystems are present in the genome, and using the information obtained to construct the metabolic network of an individual organism [23]. This Biosample is deposited in the NCBI database under the Accession number SAMN22155537 (BioProject PRJNA388578). The circular genome comparison of L. *fermentum* MC1 and D12 was generated using BRIG v0.95 [24]. The BAGEL4 server (http://bagel4.molgenrug.nl/) was used to identify gene clusters *in silico* that may be present in the genomes of L. *fermentum* MC1 and D12 and are involved in bacteriocin biosynthesis [25].

**Table 1**
Optimization of EPSs isolation from the strains L. *fermentum* MC1 and D12.

| Growth medium and conditions | Treatment | Reference |
|---|---|---|
| MRS broth +2 % *w/v* glucose, 3 days, 30 °C | cells were treated with 20 % TCA and incubated for 2 h at 4 °C under gentle agitation | [26] |
| MRS broth +2 % *w/v* glucose, 3 days, 30 °C | cells were treated with 20 mL of 2 M NaOH and shaken overnight at room temperature | [1] |
| MRS broth +2 % w/v glucose, 3 days, 30 °C | cells were treated with 0.05 M EDTA and incubated under gentle agitation for 4 h at 4 °C | [26] |
| MRS broth +2 % w/v glucose, 3 days, 30 °C | cells were treated with 0.5 % phenol and the mixture was agitated at 60 rpm at room temperature for 4 h | [27] |
| MRS agar +2 % w/v glucose, 4 days, 30 °C | cells were treated with 20 % TCA and incubated for 2 h at 4 °C under gentle agitation | [26] |
| MRS broth +2 % w/v glucose, 3 days, 30 °C | supernatant was treated with 20 % TCA and incubated for 2 h at 4 °C under gentle agitation | [26] |

### 2.3. Optimization of EPSs isolation from the strains L. fermentum MC1 and D12

To optimize the isolation of EPSs produced by strains L. *fermentum* MC1 and D12, cells grown in MRS broth (BD Difco, USA) or on MRS agar (BD Difco, USA) enriched with 2 % *w/v* glucose (Kemika, Croatia) were subjected to different treatments (Table 1). After these treatments, EPSs were obtained by protocol described in Banić et al. [17]. Finally, the purified EPSs were freeze-dried in CHRIST Alpha 1–2 LDplus (Martin Christ, Germany) and weighed on an analytical balance (Scaltec, Germany).

### 2.4. Purification of EPSs isolated from L. fermentum MC1 and D12 strains

Both EPSs, obtained by alkaline treatment of the producer strains with 2 M NaOH (Kemika, Croatia), were separated by medium pressure size-exclusion chromatography (SEC) according to protocol described in Bellich et al. [28]. Calibration of the Sephacryl S-300 HR column was achieved using pullulan standards [28]. The total amount of samples loaded on the column were 55 mg of D12 EPSs and 19 mg of MC1 EPSs which were dissolved in 12 mL and 4 mL of 0.15 M NaCl, respectively (multiple separations were performed). As reported in Fig. S1, each chromatogram is characterized by only one peak, which was divided in three parts [head (D12-H, D12-C), centre (D12—C, MC1-C), and tail (D12-T, MC1-T)], and fractions belonging to the same part were pooled together. The samples were dialyzed against water, the pH value was adjusted to neutrality and the samples were lyophilized. The following amounts of D12 EPS fractions were recovered: D12-H = 8.6 mg, D12-C = 24.1 mg and D12-T = 4.3 mg; the amounts recovered of MC1 EPS fractions were: MC1-H = 1.7 mg, MC1-C = 10.5 mg and MC1-T = 1.3 mg. Approximately 1 to 2 mg of each sample was subjected to NMR spectroscopy.

### 2.5. Composition and linkage analysis of D12 EPS

Derivatization of D12 EPS to alditol acetates and to trimethylsilyl methyl glycosides was used to establish the composition, while methylation analysis determined the position of the glycosidic linkages. About 0.5 mg were used for each procedure following the protocols described in Manna et al. [29]. GLC and GLC-MS analysis of the derivatives were performed as already reported [29]. Quantification of each component in the PMAA mixture was achieved by correcting the values of the integrated peak areas with the effective carbon response factors [30]. The absolute configuration was determined (0.5 mg of EPS) as reported in the literature [31,32].

### 2.6. NMR spectroscopy

About 2–10 mg of EPS were exchanged twice with 99.9 % $D_2O$, dissolved in 0.6 mL of the same solvent and transferred in a 5 mm NMR tube for recording NMR spectroscopy experiments on a 500 MHz VARIAN UNITY INOVA NMR spectrometer (Agilent Technologies, USA) operating at 50 °C. Chemical shifts are expressed in ppm relative to acetone (2.225 for $^{1}H$ and 31.07 ppm for $^{13}C$). NMR spectra were processed using MestreNova software.

### 2.7. Adhesion to Caco-2 cell line

Adhesion of L. *fermentum* MC1 to the Caco-2 cell line *in vitro* was performed as reported [11]. The experiments were repeated three times and the adhesion to the Caco-2 cell line was calculated using the following equation: $\Delta\log(CFU/mL) = \log(CFU/mL)_{before\ adhesion} - \log(CFU/mL)_{after\ adhesion}$.

### 2.8. Testing the antimicrobial activity by the agar well-diffusion method

The antimicrobial activity of the overnight grown culture of the strains L. *fermentum* MC1 and D12 was tested against *E. coli* 3014 and *S.* Typhimurium FP1 using the agar well-diffusion method. 100 μL of the bacterial culture of the test-microorganism ($OD_{620} = 2$) was added to 12 mL of sterile 1.5 % *w/v* nutrient agar, which was melted and cooled to 50 °C beforehand. After solidification, holes were drilled in the agar with a sterile 7 mm diameter drill and 40 μL of the antimicrobial culture supernatant was added for efficacy testing. The diameters of the inhibition zones were measured after 18 h of incubation at 37 °C.

### 2.9. Competitive exclusion assay by L. fermentum MC1 and D12 on the Caco-2 cell line

The addition of EPSs isolated from MC1 at a concentration of 0.5 and 1 mg/mL and the EPSs themselves at the same concentrations, as well as MC1 strain itself, were tested for competitive exclusion following the published protocol [33]. MC1/EPSs/MC1 + EPSs were then cultured for 1 h with a Caco-2 monolayer. The total number of viable adherent *E. coli* 3014 and *S.* Typhimurium FP1 was determined by the spot-plate method on Rapid (Biorad, USA) and XLD (Biolife, Italy) agar plates, respectively.

### 2.10. Statistical analysis

The results are showed as mean values of three separate experiments ± standard deviation (SD). Statistical significance was determined using one-way analysis of variance (ANOVA). Pairwise differences between the group means were determined using Tukey's honestly significant difference test for pairwise comparisons after analysis of variance (https://www.statskingdom.com/index.html, accessed on 11 January 2024) [34]. Images were created using GraphPad Prism v.9.4.1 (GraphPad Software, USA). Differences between samples were considered significant at $p < 0.05$.

**Table 2**
Genome characterization comparison of *Limosilactobacillus fermentum* MC1 and D12 strains using the RAST server.

| Genome data | *L. fermentum* MC1 | *L. fermentum* D12 |
|---|---|---|
| Size (bp) | 1,991,595 | 2,016,340 |
| GC content | 52.1 | 52.0 |
| N50[a] | 35,468 | 62,009 |
| L50[b] | 18 | 11 |
| Number of contigs (with PEGs) | 75 | 29 |
| Number of subsystems | 218 | 313 |
| Number of coding sequences | 2049 | 1972 |
| Number of RNAs | 40 | 64 |

[a] N50 = the sequence length of the shortest contig at 50 % of the total assembly length.
[b] L50 –=count of smallest number of contigs whose length sum makes up half of genome size.

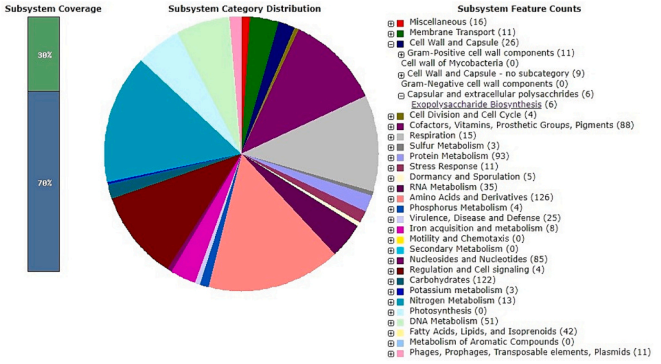


**Fig. 1.** Functional annotation of the genes of L. *fermentum* strain MC1 using the RAST server. The subsystem of the genome related to EPSs biosynthesis is highlighted in purple. (For interpretation of the references to colour in this figure legend, the reader is referred to the web version of this article.)

## 3. Results and discussion

### 3.1. Comparison of the whole genomes and genes for EPSs biosynthesis of MC1 and D12 strains

Whole-genome comparison of L. *fermentum* MC1 and D12 was performed due to the different origin of the autochthonous LAB strains, namely human and cow's milk. Furthermore, the presence of putative EPS-encoding genes in the MC1 genome was also investigated, as had already been done for the D12 strain in our previous research [11]. Genome mining of the L. *fermentum* MC1 genome was achieved using the RAST server, which revealed that it contains 1,991,595 pb distributed over 75 contigs, with the proportion of G + C base pairs being 52.1 % (Table 2). The results obtained are consistent with the average size of the LAB genome (1.3–3.3 Mb), and the proportion of G + C base pairs is consistent with previously sequenced *Limosilactobacillus fermentum* strains, which is higher than the GC content of other LAB species [35]. The number of coding sequences is also consistent with the average number of coding sequences (1700–3000) in other L. *fermentum* strains [36]. The genome size (1,991,595 bp in comparison to 2,016,340 bp for D12), G + C content (52.1 % in comparison to 52.0 % for D12) and number of coding sequences (2049 in comparison to 1972 for D12) are similar to our previously described L. *fermentum* D12 strain. On the contrary, the number of contigs (75 in comparison to 29 for D12) is higher, while the number of RNAs is lower in MC1 strain (40 in comparison to 64 for D12) (Table 2) [11].

The genome sequence of strain MC1 was annotated *in silico* to determine the subsystems associated with EPSs biosynthesis using the RAST server (Fig. 1). A subsystem related to EPSs biosynthesis was also found in other L. *fermentum* strains [37], including strain D12 [11].

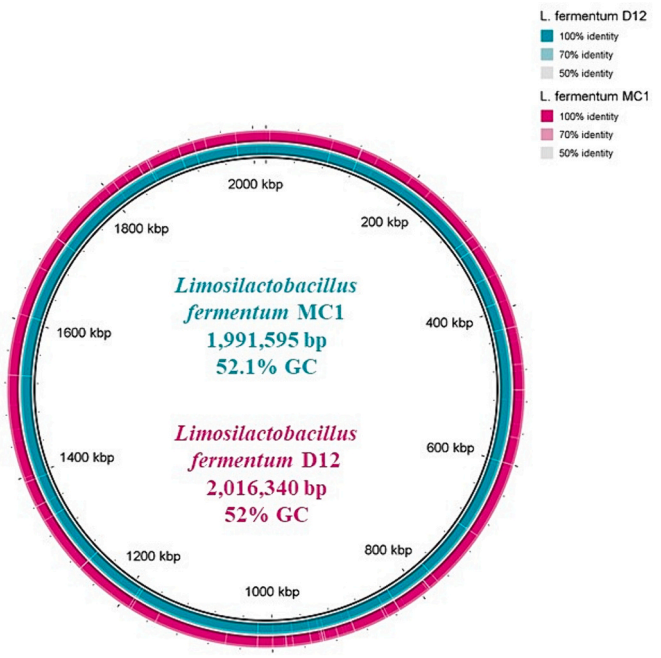


**Fig. 2.** Graphical genome comparison map of the D12 strain (pink) with the closely related MC1 strain (green) using the BRIG tool. The intensity of the corresponding strains colour in the legend indicates the pairwise genomic sequence similarity according to blastn. (For interpretation of the references to colour in this figure legend, the reader is referred to the web version of this article.)

To point out the differences between the MC1 and D12 genomes, a genome comparison was carried out using BRIG (BLAST Ring Image Generator), a cross-platform desktop application that allows visualization of BLAST comparisons with reference sequences using genomic data [24]. The results show a high degree of overlapping identity between the two genomes (Fig. 2), which was expected as they belong to the same species, including some genes involved in EPSs production *via* the Wzx/Wzy-dependent pathway (Table 3). Although there is a high degree of similarity, the MC1 genome contains *epsIIG* and *epsF* involved in EPSs biosynthesis, which were not detected in the D12 genome, while the D12 genome harbours *epsC*', which is involved in transport and polymerization of EPSs and which was not detected in the MC1 genome.

Most LAB strains, including L. *fermentum* MC1 (Table 3), produce EPSs *via* the Wzx/Wzy-dependent pathway [38], which is divided into 5 steps [39]. Eight genes encoding the phosphotransferase system (PTS), which simultaneously transports and phosphorylates monosaccharides or oligosaccharides, were found in the genome of strain MC1 (results not shown). Genes encoding for sugar activating enzymes, phosphoglucomutase (*pgm*), galactose-1-phosphate uridylyltransferase (*galT*), UDP-glucose-4-epimerase (*galE*) and dTDP-glucose-4,6-dehydratase (*rfbB*) were detected; the latter is the first of two enzymes involved in rhamnose biosynthesis which was not found in any of the isolated EPSs. Genes encoding for glycosyltransferases [priming undecaprenyl-phosphate galactosephosphotransferase (EpsE), exopolysaccharide biosynthesis glycosyltransferase (EpsF), and putative glycosyltransferase (EpsIIG)], whose activity builds the repeating units, and genes for the flippase (Wzx) and the polymerase (Wzy) were found in the MC1 genome. In addition, genes encoding transcriptional regulator (EpsA), manganese-dependent protein-tyrosine phosphatase (EpsB), tyrosine-protein kinase transmembrane modulator (EpsC), tyrosine-protein kinase (EpsD), and acetyltransferase involved in the biosynthesis and regulation of EPSs were found in the MC1 genome. As expected from genomic data and EPS structures, these data are similar to those collected for D12 strain [11].

**Table 3**
Genes of *L. fermentum* MC1 involved in exopolysaccharides production *via* Wzx/Wzy-dependent pathway.

| Gene | Start | Stop | Strand | Function |
|---|---|---|---|---|
| Precursor Activation | | | | |
| *pgm* | 14,818 | 13,094 | – | Phosphoglucomutase (EC 5.4.2.2) |
| *galT* | 25,224 | 26,678 | + | Galactose-1-phosphate uridylyltransferase (EC 2.7.7.10) |
| *galE* | 32,393 | 33,388 | + | UDP-glucose 4-epimerase (EC 5.1.3.2) |
| *galU* | 75,845 | 76,756 | + | UTP-glucose-1-phosphate uridylyltransferase (EC 2.7.7.9) |
| *glf* | 8338 | 9459 | + | UDP-galactopyranose mutase (EC 5.4.99.9) |
| *rfbB* | 26,346 | 27,278 | + | dTDP-glucose 4,6-dehydratase (EC 4.2.1.46) |
| Exopolysaccharide biosynthesis | | | | |
| *epsA* | 3267 | 2266 | – | Cell envelope-associated transcriptional attenuator LytR-CpsA-Psr, subfamily F2 |
| *epsB* | 711 | 1 | – | Manganese-dependent protein-tyrosine phosphatase (EC 3.1.3.48) |
| *epsB'* | 11,520 | 11,329 | – | Manganese-dependent protein-tyrosine phosphatase (EC 3.1.3.48) |
| *epsC* | 2266 | 1496 | – | Tyrosine-protein kinase transmembrane modulator EpsC |
| *epsD* | 1478 | 738 | – | Tyrosine-protein kinase EpsD (EC 2.7.10.2) |
| *epsE* | 4971 | 5624 | + | Undecaprenyl-phosphate galactosephosphotransferase (EC 2.7.8.6) |
| *epsF* | 10,629 | 9523 | – | Exopolysaccharide biosynthesis glycosyltransferase EpsF (EC 2.4.1.-) |
| *epsIIG* | 23,619 | 24,527 | + | EpsIIG, Putative glycosyltransferase |
| *gt* | 5636 | 6397 | + | Glycosyltransferase |
| *at* | 10,890 | 11,948 | + | Membrane protein, putative actyltransferase |
| Transport and polymerization | | | | |
| *wzx* | 9462 | 10,880 | + | Membrane protein involved in the export of O-antigen, teichoic acid lipoteichoic acids |
| *wzy* | 6408 | 7631 | + | Hypothetical protein, polymerase |

### 3.2. Optimization of isolation and purification of EPSs biosynthesized by L. fermentum MC1 and D12 strains

Different protocols have been assessed to isolate EPSs of good purity: growth of the strains on solid and in liquid MRS medium, followed by isolation of the EPSs from i) the supernatant by TCA treatment, ii) the cells by EDTA treatment, iii) the cells by phenol treatment, iv) the cells by TCA treatment. However, the best results in terms of purity and yield were obtained by cultivating the strains in liquid MRS broth supplemented with 2 % glucose and isolating the EPSs from the cell surface after treatment with 2 M NaOH.

The isolated MC1 and D12 EPSs were subjected to $^{1}$H NMR spectroscopy, which revealed almost identical 1D spectra, the only difference being some very low intensity anomeric resonances in MC1 sample, thus suggesting production of the same main polysaccharides by these two strains (Fig. S2). Moreover, the anomeric regions showed resonances with very different integration areas, indicating the presence of more than one polysaccharide. The EPSs samples were subjected to size-exclusion chromatography on a Sephacryl S-300 HR column and both eluted as a single peak with a molecular mass of approximately 9 kDa, as determined after calibration with pullulan standards. In order to separate the different polysaccharides, each peak was divided into three parts (head (H), center (C), and tail (T), Fig. S1), and each fraction was subjected to $^{1}$H NMR spectroscopy. As shown in Figs. S3 and S4, the three fractions of each EPSs have identical $^{1}$H NMR spectra, indicating that SEC chromatography was not successful in separating the different components.

Since $^{1}$H NMR spectra showed that the main resonances were

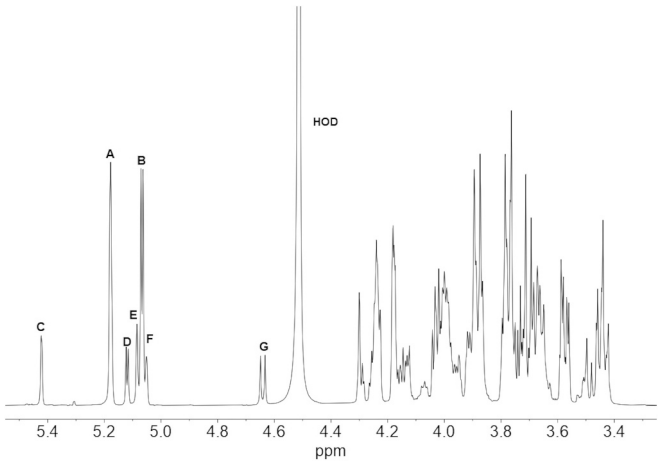


**Fig. 3.** $^{1}$H NMR spectrum of D12 EPS recorded in $D_2O$, at 500 MHz and 50 °C. Anomeric signals are indicated.

identical in all fractions of both samples, D12-C fraction, being the most abundant, was used for in depth structural investigation, and simply named D12 EPS.

### 3.3. Composition and linkage analysis of D12 EPSs

Composition analysis was carried out by GLC and GLC-MS after chemical derivatization of the D12 EPSs to alditol acetates and trimethylsylil methyl-glycosides. Both methods showed only Gal and Glc in the relative molar ratios 1.2 : 1.0. The absolute configuration was determined to be D for both sugars. The determination of the glycosidic linkages was achieved by GLC-MS analysis of the partially methylated alditol acetates which identified: t-Glc*p* : 3-Gal*f* : 3-Glc*p* : 6-Gal*f* : 2,6-Gal*f* in the molar ratios 1.00 : 0.10 : 0.14 : 0.18 : 0.51.

### 3.4. NMR spectroscopy of D12 EPSs

The $^{1}$H NMR spectrum of the anomeric region of D12 EPS (Fig. 3) shows two more intense resonances at 5.18 (A) and 5.07 (B) ppm and five less intense ones at 5.24 (C), 5.12 (D), 5.08 (E), 5.05 (F) and 4.64 (G) ppm. The $^{1}$H NMR spectrum was consistent in different preparation batches with the peaks' areas in the molar ratio of 1 for A and B, 0.2 for C, D, E, G, while peak F always had an integration value <0.2. As expected, these different integration values indicated the presence of three different EPSs: one composed of residues A and B, the second one containing C, D, E, and G, and possibly a homopolymer composed only of residue F. In a previous article [11] it was established that the main components (A and B) correspond to 2,6-Gal*f* and t-Glc*p*, respectively. $^{1}$H—$^{1}$H and $^{13}$C—$^{1}$H 2D experiments were recorded to establish the structure of the polysaccharides. First of all, the resonances belonging to the two most abundant spin systems, A and B, were considered. The COSY spectrum (data not shown) established the H2 resonances for each spin system, while the TOCSY experiment gave H1 to H4 for A spin system, and H1 to H6 for B spin system (Fig. S5). Inspection of the HSQC spectrum (Fig. 4A) resulted in the complete $^{1}$H—$^{13}$C assignments for each spin system, and the data are reported in Table 4. C2 and C6 of residue A are deshielded with respect to a not-linked β-Gal*f* residue [40], thus indicating that they are the site of glycosidic linkages, while the α-Glc*p* chemical shifts are in agreement with a t-Glc. An HMBC spectrum (Fig. 4B) showed both intra- and inter-residue connectivities; among the latter β-Gal*f* H1 (5.18 ppm) was correlated to C6 (70.1 ppm) of the same spin system, thus establishing that the Eps main chain is constituted by 1–6 linked β-Gal*f* residues, while H1 of t-α-Glc*p* (5.07 ppm) was correlated to β-Gal*f* C2 (87.5 ppm) (Table 5). At the same time, anomeric carbon – ring proton correlations confirmed the linkages. Therefore, the structure of the main EPS produced by L. *fermentum* D12, named D12 EPS I, in the growth conditions adopted is as follows (Scheme 1):

Regarding the other spin systems C - F, by increasing the intensity of the 2D spectra, it was possible to obtain the complete assignments of the chemical shifts for each spin system. The COSY spectrum (data not shown) established the H2 resonances for each spin system, while the TOCSY experiment (Fig. S6) gave most of the protons. Inspection of the HSQC spectrum (Fig. 5) resulted in $^{1}$H—$^{13}$C determination for each spin system, and the data are reported in Table 4. The resonances for C2 and C6 of C, C3 of E and G, and C6 of F, and C-4 of D were displaced downfield with respect to their shifts in non-substituted monosaccharides [40], demonstrating the glycosylation pattern of the RU. The HMBC spectrum (Fig. 6A and B) showed intra-residue connectivities which confirmed the chemical shifts assignments and the following inter-residue connectivities (Table 5): H1 of 2,6-β-D-Gal*f* (5.42 ppm) to C3 (83.2 ppm) of 3-β-D-Glc*p*, C1 of 2,6-β-D-Gal*f* (107.5) to H3 (3.67 ppm) of 3-β-D-Glc*p*, H1 (5.12 ppm) of α-D-Glc*p* to C2 (87.6 ppm) of 2,6-β-D-Gal*f*, C1 of α-D-Glc*p* to H2 (4.24 ppm) of 2,6-β-D-Gal*f*, H1 (5.08 ppm) of 3-β-D-Gal*f* to C6 (70.2 ppm) of 2,6-β-D-Gal*f*, H1 (4.64 ppm) of 3-β-D-Glc*p* to C3 (85.4 ppm) of 3-β-D-Gal*f*, H1 (102.9 ppm) of 3-β-D-Glc*p* to H3 (4.29 ppm) of 3-β-D-Gal*f*, H1 (5.05 ppm) of 6-β-D-Gal*f* to its C6 (70.2 ppm), and C1 (108.7 ppm) of 6-β-D-Gal*f* to its H6 (3.88, and 3.64 ppm). All these inter-residues connectivities established that the five spin systems compose the following two exopolysaccharides, named

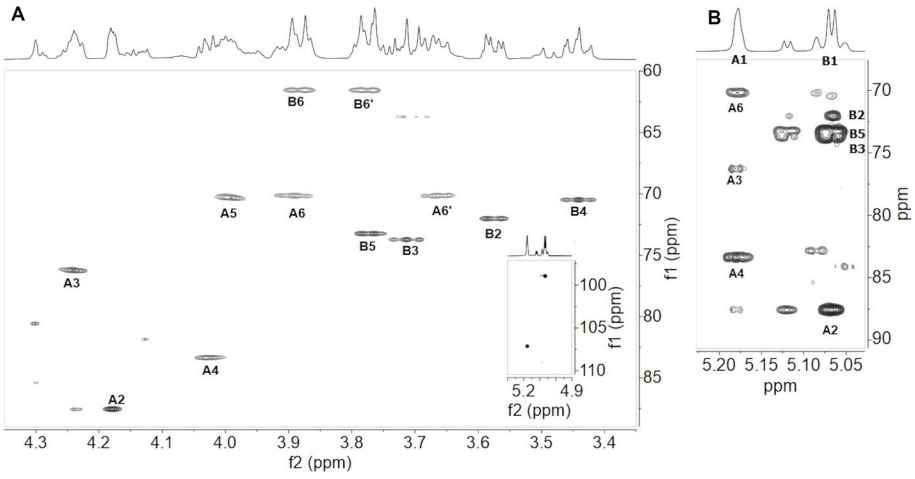


**Fig. 4.** HSQC (4 A) and HMBC (4B) spectra of D12 EPSs recorded in $D_2O$, at 500 MHz and 50 °C showing only the cross peaks related to residues A and B. Proton/carbon crosspeaks are labelled according to the corresponding residue, as in Table 4.

**Table 4**
$^{1}H$ and $^{13}C$ chemical shift assignments of the seven sugars composing the different EPSs produced by *Limosilactobacillus fermentum* D12 recorded at 500 MHz and 50 °C. Grey cells indicate chemical shifts of carbon atoms involved in glycosidic linkages.

| Residue | Nucleus | Chemical shifts (ppm) [a] | | | | | |
|---|---|---|---|---|---|---|---|
| | | 1 | 2 | 3 | 4 | 5 | 6 |
| **A** | $^{1}H$ | 5.18 | 4.18 | 4.24 | 4.02 | 3.99 | 3.89 - 3.67 |
| **→2,6)-β-D-Gal*f*-(1→** | $^{13}C$ | 107.1 | 87.5 | 76.2 | 83.4 | 70.3 | 70.1 |
| **B** | $^{1}H$ | 5.07 | 3.57 | 3.71 | 3.44 | 3.76 | 3.88 – 3.78 |
| **α-D-Glc*p*-(1→** | $^{13}C$ | 98.9 | 72.0 | 73.8 | 70.5 | 73.3 | 61.5 |
| **C** | $^{1}H$ | 5.42 | 4.24 | 4.24 | 4.14 | 4.01 | 3.89 - 3.67 |
| **→2,6)-β-D-Gal*f*-(1→** | $^{13}C$ | 107.5 | 87.6 | 76.3 | 83.2 | 70.3 | 70.2 |
| **D** | $^{1}H$ | 5.12 | 3.58 | 3.72 | 3.45 | 3.78 | 3.93 – 3.75 |
| **α-D-Glc*p*-(1→** | $^{13}C$ | 98.8 | 72.1 | 73.8 | 70.6 | 73.3 | 61.7 |
| **E** | $^{1}H$ | 5.08 | 4.30 | 4.29 | 4.16 | 3.96 | 3.72 - 3.68 |
| **→3)-β-D-Gal*f*-(1→** | $^{13}C$ | 109.0 | 80.6 | 85.4 | 82.8 | 71.3 | 63.7 |
| **F** | $^{1}H$ | 5.05 | 4.13 | 4.07 | 4.01 | 3.97 | 3.88 - 3.64 |
| **→6)-β-D-Gal*f*-(1→** | $^{13}C$ | 108.7 | 81.9 | 77.7 | 84.1 | 70.3 | 70.2 |
| **G** | $^{1}H$ | 4.64 | 3.44 | 3.67 | 3.49 | 3.50 | 3.93 - 3.76 |
| **→3)-β-D-Glc*p*-(1→** | $^{13}C$ | 102.9 | 73.9 | 83.2 | 69.0 | 76.7 | 61.7 |

[a]Chemical shifts are given relative to internal acetone (2.225 ppm for $^{1}H$ and 31.07 ppm for $^{13}C$).

**Table 5**
anomeric proton – ring carbon correlations and anomeric carbon – ring proton correlations determined with the HMBC experiment.

| Residues | Anomeric Proton (ppm) | Correlated to $^{13}C$ (ppm) | Anomeric Carbon (ppm) | Correlated to $^{1}H$ (ppm) |
|---|---|---|---|---|
| →2,6)-β-D-Gal*f*-(1→(**A**) | **A1** (5.18) | **A6** (70.1) | **A1** (107.1) | **A6** (3.89) |
| | | **A3** (76.2) | | **A6'** (3.67) |
| | | **A4** (83.4) | | **A2** (4.18) |
| α-D-Glc*p*-(1→(**B**) | **B1** (5.07) | **B2** (72.0) | **B1** (98.9) | **B2** (3.57) |
| | | **B5** (73.3) | | **B3** (3.71) |
| | | **B3** (73.8) | | **B5** (3.76) |
| | | **A2** (87.5) | | **B6** (3.88) |
| | | | | **A2** (4.18) |
| →2,6)-β-D-Gal*f*-(1→(**C**) | **C1** (5.42) | **C3** (76.3) | **C1** (107.5) | **C2** (4.24) |
| | | **G3** (83.2) | | **G3** (3.67) |
| | | **C2** (87.6) | | |
| α-D-Glc*p*-(1→(**D**) | **D1** (5.12) | **D2** (72.1) | **D1** (98.8) | **D2** (3.58) |
| | | **D5** (73.3) | | **D3** (3.72) |
| | | **D3** (73.8) | | **D5** (3.78) |
| | | **C2** (87.6) | | **C2** (4.24) |
| →3)-β-D-Gal*f*-(1→(**E**) | **E1** (5.08) | **C6** (70.2) | | |
| | | **E4** (82.8) | | |
| | | **E3** (85.4) | | |
| →6)-β-D-Gal*f*-(1→(**F**) | **F1** (5.05) | **F6** (70.2) | **F1** (108.7) | **F6** (3.88) |
| | | **F3** (77.7) | | **F6'** (3.64) |
| | | **F4** (84.1) | | |
| →3)-β-D-Glc*p*-(1→(**G**) | **G1** (4.64) | **G5** (76.7) | **G1** (102.9) | **G2** (3.44) |
| | | **G3** (83.2) | | **E3** (4.29) |
| | | **E3** (85.4) | | |

D12 EPS II and III, respectively (Scheme 2):

The possible presence of base-labile substituents, like acetyl groups, could not be determined due to the use of NaOH for EPSs purification. Moreover, NMR chemical shifts were confirmed using the simulation

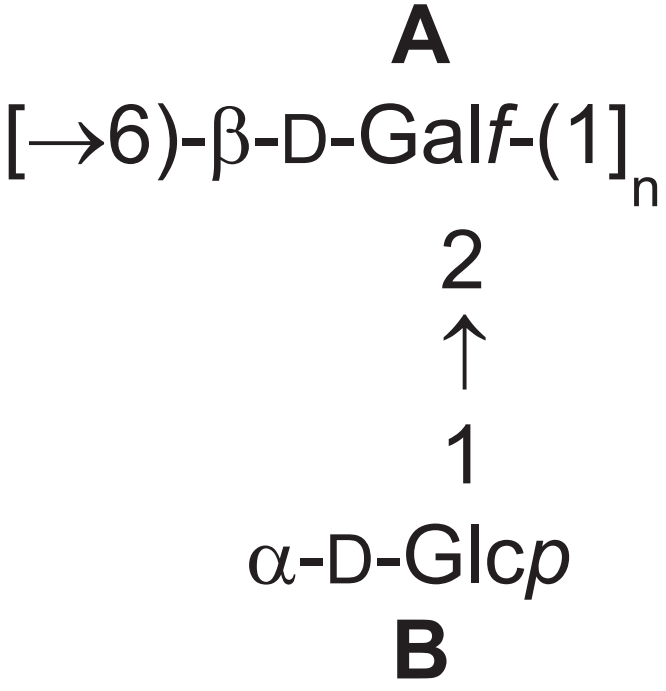


**Scheme 1.** structure of the repeating unit of D12 EPS I.

tool for $^{13}C$ [41,42] nucleus at the Carbohydrate Structure Database (CSDB) [43], the CSDB structural ranking tool [44], and empirical chemical shift simulation [45], fully supporting the proposed structures (Tables S1-S3).

### 3.5. NMR spectroscopy of MC1 EPSs

In order to undoubtedly prove that MC1 and D12 EPSs are identical,

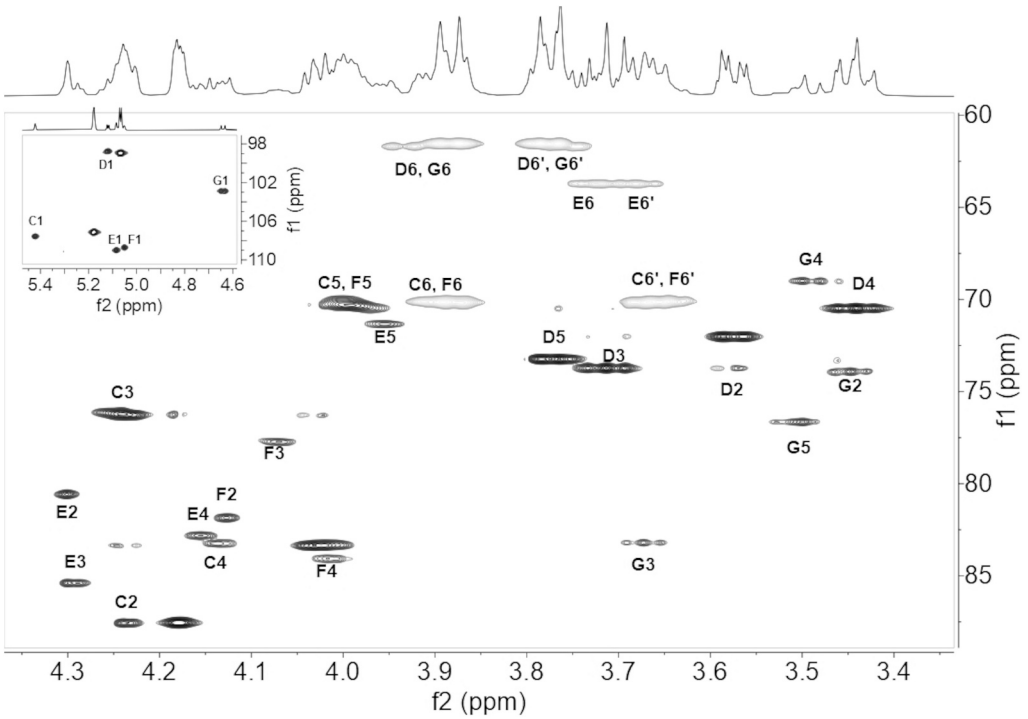


**Fig. 5.** Higher intensity HSQC plot of D12 EPSs recorded in $D_2O$, at 500 MHz and 50 °C. Proton/carbon crosspeaks are labelled according to the corresponding residue, as in Table 4 (only cross-peaks related to spin system from C to G are shown).

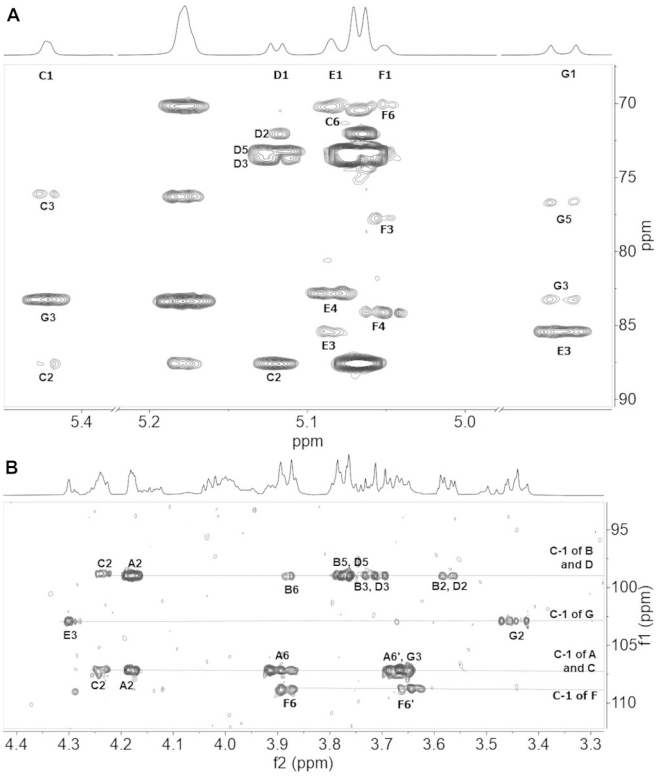


**Fig. 6.** Higher intensity HMBC plot of D12 EPSs recorded in $D_2O$, at 500 MHz and 50 °C. Proton/carbon crosspeaks are labelled according to the corresponding residue, as in Table 4 (only cross-peaks related to spin system from C to G are shown).

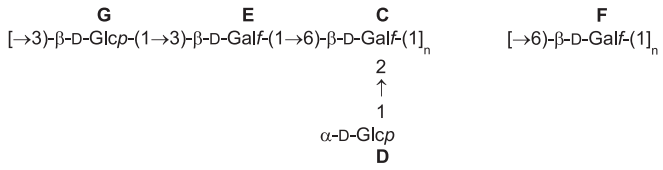


**Scheme 2.** Structure of the repeating units of D12 EPS II (left) and D12 EPS III (right).

an HSQC experiment of MC1 EPSs was recorded. The spectrum (Fig. S7) is identical to that of D12 EPS, thus confirming the identity of the EPSs produced by the two strains when isolated using NaOH.

### 3.6. Comparison of the functional properties of L. fermentum MC1 and D12 strains

Although EPS-producing LAB are implemented in the production of various dairy products due to their interesting technological properties, there are not many reports on the functional probiotic properties of the EPSs extract itself, especially for the genus *Lactobacillus* [18]. Many researchers have confirmed numerous functional roles of EPSs, such as antioxidant, antibacterial, immunoregulatory, antitumor, anticoagulant and antiviral effects and influence on the health of the host's intestinal tract [9]. Therefore, addition of these strains as probiotic supplement could help to stabilize an imbalanced gut microbiota, as the presence of these bacteria in the gut microbiota is related to a healthy state of the host [14]. Many health-promoting effects of probiotic strains are connected to their ability to adhere to the intestinal mucosa, a necessary prerequisite for the colonization of the gastrointestinal tract (GIT), which gives the cell a competitive advantage and is also one of the main criteria for the selection of probiotic strains. Bacterial adhesion ability varies between strains depending on the properties of the cell surface, and it is hypothesized that exopolysaccharides, among other molecules, might influence the ability of the producing bacteria to adhere to

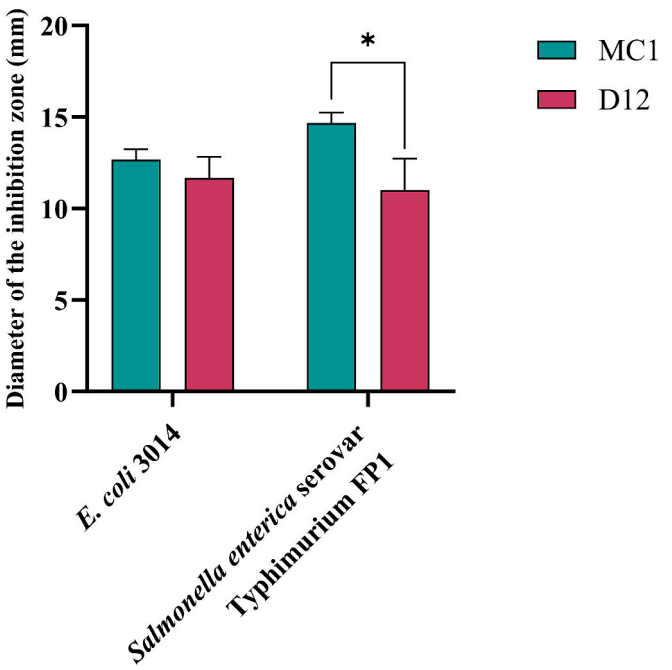


**Fig. 7.** Inhibition of *Escherichia coli* 3014 and *Salmonella enterica* serovar Typhimurium FP1 by L. *fermentum* MC1 (green) and D12 (red), expressed as the diameter of the inhibition zones around the grown cultures (cm). The error bars represent the standard deviations of the mean values of the results from three replicates. *Statistical difference (*$p < 0.05$). (For interpretation of the references to colour in this figure legend, the reader is referred to the web version of this article.)

different structures of the intestinal tract and form a biofilm [46]. Butorac et al. [11] have already demonstrated the functional properties of the D12 strain, showing its ability to adhere to Caco-2 intestinal epithelial cells and extracellular matrix proteins and to survive freeze-drying and unfavorable conditions like simulated GIT environment. Therefore, the functional properties of the MC1 strain were also investigated using Caco-2 cells as an *in vitro* model for predicting adhesion ability to intestinal epithelial cells. The results showed that the MC1 strain adhered better to Caco-2 cells than the D12 strain ($p < 0.017$) [11] as shown by its lower Δlog (CFU/mL) value (2.4 ± 0.13 for the MC1 strain compared to 3.63 ± 0.53 for the D12 strain), thus favoring the MC1 strain as a potentially adherent probiotic strain. It is possible that the EPSs of the D12 strain mask some of the microbial cell surface adhesins involved in adhesion to intestinal cells, whereas the EPSs of the MC1 strain do not have the same effect. Additionally, some other surface molecules, which can be strain-specific, like cell surface proteins, may also be involved in adhesion mechanisms [22,33,47].

Antibacterial activity is one of the important features of probiotic strains, as various antimicrobial compounds such as organic acids (lactic and acetic acid), hydrogen peroxide, ethanol, diacetyl, acetaldehyde, acetoin, carbon dioxide, reuterin, reutericyclin and bacteriocins can be produced and can exhibit strong antagonistic activity against many Gram-positive and Gram-negative bacteria, including pathogens and those causing spoilage [48]. Therefore, the ability of MC1 and D12 to inhibit the growth of potentially pathogenic *E. coli* 3014 and *S.* Typhimurium FP1 was examined. The results showed (Fig. 7) that both L. *fermentum* strains inhibited the growth of these two species to a certain extent. Strain MC1 showed a stronger antagonistic activity towards *S.* Typhimurium FP1, as the inhibition diameter was significantly higher ($p < 0.05$) than that of strain D12. However, no statistical significance between the two examined L. *fermentum* strains was detected when assessing the inhibition capacity of *E. coli* 3014 growth. This effect is not necessarily due to lactic acid, the main antibacterial metabolite of LAB, but can also be enhanced by other metabolites, including strain-specific feature like bacteriocin production. An *in silico* analysis of MC1 and D12 genomes performed using BAGEL4 software showed that only the MC1 strain harbours a gene cluster for bacteriocin production (Fig. 8), with 37.013 % sequence similarity (e-value = $1.5 \times 10^{-23}$) to enterolysin A, a class IV bacteriocins usually produced by some *Enterococcus faecalis* strains [49]. These results support our findings that strain MC1 has better antimicrobial activity against *S.* Typhimurium FP1, since enterolysin A can increase the permeability of the outer membrane of Gram-negative pathogens. Recent literature supports our findings, since production of enterolysin A was reported in other LAB strains, including L. *fermentum* [50,51].

In addition to various proteins present on the surface of the bacterial cell, extracellular metabolites such as EPSs can also be involved in adhesion and thus in competitive exclusion, which are also prerequisites for a particular strain to be considered a probiotic [17,22,33,52]. Moreover, the presence of heterologous EPS might reduce the adhesion of pathogenic bacteria to intestinal cells due to the covering of surface adhesins and contribute to their exclusion from the intestine [15]. Moreover, the presence of heterologous EPS might reduce the adhesion of pathogenic bacteria to intestinal cells due to the shielding of surface adhesins and contribute to their exclusion from the intestine. Since strain MC1 showed a better adhesion capacity to the Caco-2 cell line and a stronger growth inhibition of *S.* Typhimurium FP1, the role of EPSs isolated from the MC1 strain in the competitive exclusion of *E. coli* 3014 and *S.* Typhimurium FP1 was investigated. For this purpose, the Caco-2 cell line was pre-incubated with 0.5 and 1 mg/mL EPSs with or without the addition of MC1 cells, or with MC1 cells alone, followed by incubation with *E. coli* 3014 or *S.* Typhimurium FP1 (Fig. 9). It was found that the exclusion of *E. coli* 3014 from Caco-2 cells was the greatest with 1 mg/mL EPSs, with or without MC1 cells, in comparison to the adhered *E. coli* 3014 in the control (without MC1/EPS incubation). On the contrary, the competitive exclusion of *S.* Typhimurium FP1 was not statistically significant. Our results regarding the competitive exclusion of *E. coli* 3014 are similar to those of Liu et al. [14], who revealed that 1 mg/mL of EPSs isolated from *Lactobacillus plantarum* WLPL04 can significantly prevent the adhesion of *Escherichia coli* O157:H7 to HT-29 cells.

The findings in this study contribute to a better understanding of EPSs in the probiotic functionality of L. *fermentum* strains, but the exact mechanisms of action are not yet clear. The results obtained in this paper suggest a potential use of these strains as probiotics due to their antimicrobial activity against potentially pathogenic bacteria and adhesion

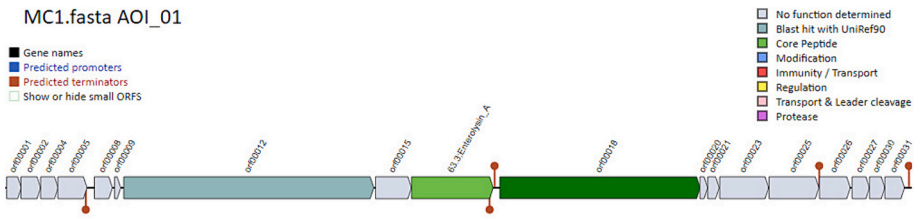


**Fig. 8.** Bacteriocin cluster found in the genome of L. *fermentum* MC1 with the position of the bacteriocin sequence in light green. (For interpretation of the references to colour in this figure legend, the reader is referred to the web version of this article.)

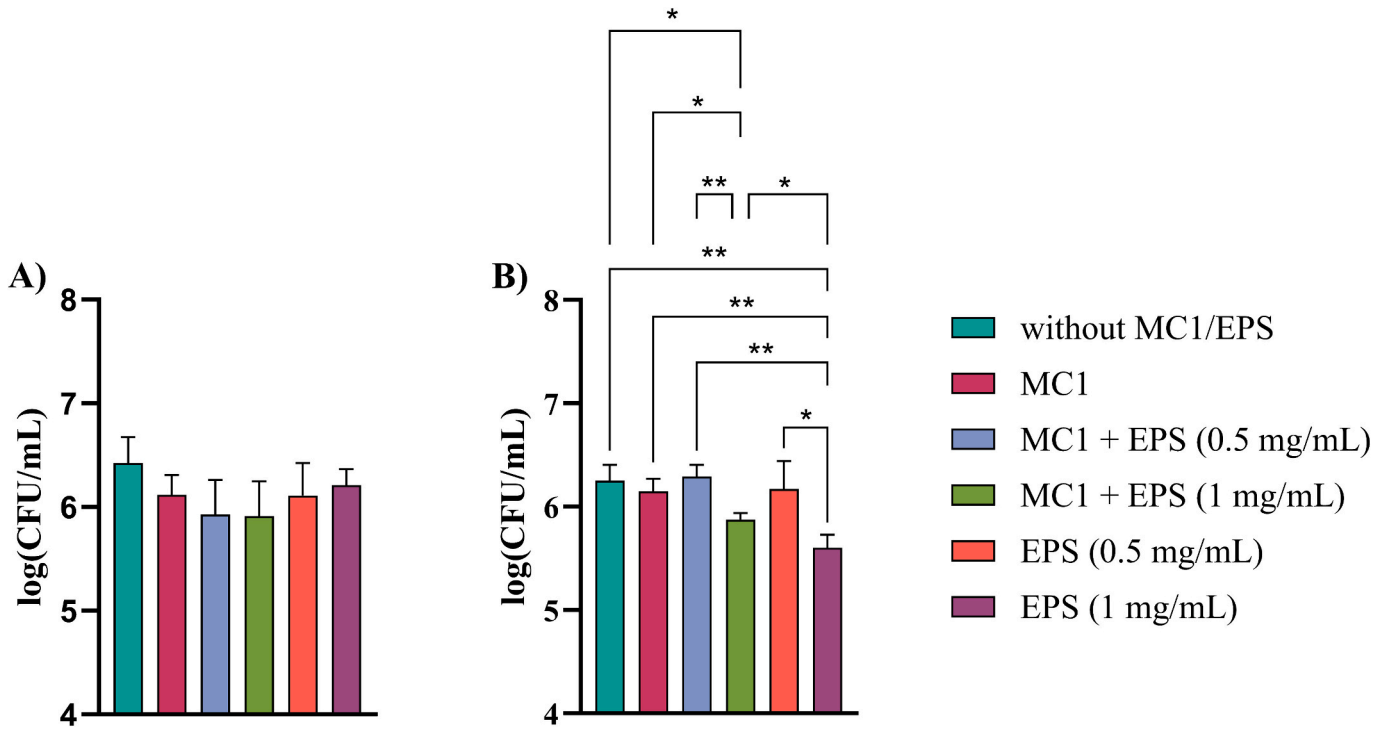


**Fig. 9.** Competitive exclusion of a) *Salmonella enterica* serovar Typhimurium FP1 and b) *Escherichia coli* 3014 after pre-incubation of Caco-2 cells with 0.5 and 1 mg/mL EPSs; 0.5 and 1 mg/mL EPS and L. *fermentum* MC1 cells and with L. *fermentum* MC1 cells alone. The error bars represent the standard deviations of the mean values of the results of three replicates. *Significantly different (*$p < 0.05$; **$p < 0.01$).

to intestinal epithelial cells. Further studies are necessary to evaluate the potential health-promoting effects such as microbiome modulatory and immunomodulatory activity of the MC1 and D12 strains, as well as their EPSs, through *in vivo* experiments on experimental animals. In addition, micro- and nanoencapsulation methods with different potential protective matrices will be investigated to improve the survival of EPS-producing strains during freeze-drying, storage and under unfavorable conditions in the GIT and to ensure their probiotic effect *in vivo*.

## 4. Conclusion

The WGS results showed that the L. *fermentum* MC1 genome differs slightly from that of D12 strain. Characterization of the produced EPSs, isolated from the cell surface with 2 M NaOH, revealed that both strains biosynthesized a mixture of three different polymers when cultivated in liquid MRS broth enriched with 2 % glucose. The structures identified are similar to those reported for *Lactobacillus fermentum* Lf2 by Ahmed et al. [53] who described a mixture of two EPSs: a more abundant EPS similar to D12 EPS I, except for the non-stoichiometric glucosylation of the Gal*f* residue, and a less abundant EPS identical to EPS II described in this manuscript. Also, Ahmed et al. [53] found a 6-linked Gal*f* residue which was assigned to the non glucosylated Gal*f* of the main polysaccharide. Moreover, the $^{1}$H NMR spectrum of MC1 EPSs shows anomeric resonances unique to this sample (Fig. S2 and S4), even if they have a very low intensity, suggesting that MC1 biosynthesizes polysaccharides which are not produced by D12, in line with the genetic findings and functional experiments. According to the results obtained, the EPSs isolated from L. *fermentum* MC1 contribute to its probiotic functionality in terms of better competitive exclusion of *E. coli* 3014. Better antimicrobial activity of MC1 against *S.* Typhimurium FP1 with respect to D12 was also proved and it was hypothesized to be due to a bacteriocin, since a gene cluster for its production was found in MC1 only.

By analyzing the genes involved in EPS biosynthesis, it is difficult to draw conclusions about their influence on the functional properties of the producer strains. In addition to EPSs, other biomolecules produced by the cell also play a role in the functional properties of the bacterial strains such as adhesion and antimicrobial activity. The main difference between the two L. *fermentum* strains examined is that only MC1 produces bacteriocins, which contribute to antimicrobial activity as a functional property. Regarding the role of EPSs in adhesion, it is known that other surface molecules, which may contain lipid and protein structures in addition to carbohydrates in their chemical composition, also play a role. Therefore, further detailed characterization of the genomes of L. *fermentum* MC1 and D12 strains and of other potential biomolecules, apart from EPSs, which may contribute to the functional properties of the tested strains is required.

## Funding

The Croatian Science Foundation funded this research through the projects IP-2014-09-7009 (“Probiotics and starter cultures-surface proteins and bacteriocins”) and IP-2019-04-2237 (“Potential therapeutic biomolecules of next-generation probiotics”). The authors acknowledge the financial support from the University of Zagreb, Croatia and the equipment procured within the project “Bioprospecting of the Adriatic Sea” (KK.01.1.1.01.0002), granted to the Scientific Centre of Excellence for Marine Bioprospecting (BioProCro) at the Ruđer Bošković Institute, Zagreb, Croatia. Also, PhD student Nina Čuljak received FEMS Research and Training Grant (FEMS-GO-2021-034) for early career scientists.

## CRediT authorship contribution statement

**Nina Čuljak:** Writing – review & editing, Writing – original draft, Visualization, Investigation, Formal analysis, Conceptualization. **Barbara Bellich:** Validation, Methodology, Investigation. **Alice Pedroni:** Investigation. **Katarina Butorac:** Investigation, Formal analysis, Data curation. **Andreja Leboš Pavunc:** Writing – review & editing, Validation, Project administration. **Jasna Novak:** Writing – review & editing, Supervision. **Martina Banić:** Writing – review & editing, Formal

analysis, Data curation. **Jagoda Šušković:** Writing – review & editing, Supervision. **Paola Cescutti:** Writing – review & editing, Writing – original draft, Visualization, Validation, Methodology, Conceptualization. **Blaženka Kos:** Writing – review & editing, Supervision, Funding acquisition, Conceptualization.

## Declaration of competing interest

The authors declare that they have no known competing financial interests or personal relationships that could have appeared to influence the work reported in this paper.

## Data availability

Data will be made available on request.

## Acknowledgments

The authors would like to thank associate professor Ksenija Durgo from University of Zagreb Faculty of Food Technology and Biotechnology, Laboratory for Biology and Microbial Genetics for preparing Caco-2 cell line for the adhesion and competitive exclusion procedure. Prof. Neil Ravenscroft (Department of Chemistry, University of Cape Town) is gratefully acknowledged for useful discussion about NMR spectra interpretation.

## Appendix A. Supplementary data

Supplementary data to this article can be found online at https://doi.org/10.1016/j.ijbiomac.2024.133215.

## References

[1] M. Ferrari, L. Hameleers, M.C. Stuart, M.M. Oerlemans, P. de Vos, E. Jurak, M. T. Walvoort, Efficient isolation of membrane-associated exopolysaccharides of four commercial bifidobac- terial strains, Carbohydr. Polym. 278 (2022) 118913, https://doi.org/10.1016/j.carbpol.2021.118913.

[2] G.M. Daba, M.O. Elnahas, W.A. Elkhateeb, Contributions of exopolysaccharides from lactic acid bacteria as biotechnological tools in food, pharmaceutical, and medical applications, Int. J. Biol. Macromol. 173 (2021) 79–89, https://doi.org/10.1016/j.ijbiomac.2021.01.110.

[3] H. Yildiz, N. Karatas, Microbial exopolysaccharides: resources and bioactive properties, Process Biochem. 72 (2018) 41–46, https://doi.org/10.1016/j.procbio.2018.06.009.

[4] A. Hussain, K.M. Zia, S. Tabasum, A. Noreen, M. Ali, R. Iqbal, M. Zuber, Blends and composites of exopolysaccharides; properties and applications: a review, Int. J. Biol. Macromol. 94 (2017) 10–27, https://doi.org/10.1016/j.jchromb.2003.12.023.

[5] A. Suresh Kumar, K. Mody, B. Jha, Bacterial exopolysaccharides – a perception, J. Basic Microb. 47 (2) (2007) 103–117, https://doi.org/10.1002/jobm.200610203.

[6] Food and Agriculture Organization of the United Nations/World Health Organization, Report of a Joint FAO/WHO Expert Consultation on Evaluation of Health and Nutritional Properties of Probiotics in Food Including Powder Milk with Live Lactic Acid bacteria, Córdoba, Argentina, 2001, pp. 19–20.

[7] D. Deo, D. Davray, R. Kulkarni, A diverse repertoire of exopolysaccharide biosynthesis gene clusters in *Lactobacillus* revealed by comparative analysis in 106 sequenced genomes, Microorganisms 7 (10) (2019) 444, https://doi.org/10.3390/microorganisms7100444.

[8] J. Schmid, Recent insights in microbial exopolysaccharide biosynthesis and engineering strategies, Curr. Opin. Biotech. 53 (2018) 130–136, https://doi.org/10.1016/j.copbio.2018.01.005.

[9] J. Angelin, M. Kavitha, Exopolysaccharides from probiotic bacteria and their health potential, Int. J. Biol. Macromol. 162 (2020) 853–865, https://doi.org/10.1016/j.ijbiomac.2020.06.190.

[10] J. Zheng, S. Wittouck, E. Salvetti, C.M. Franz, H.M. Harris, P. Mattarelli, P. W. O'Toole, B. Pot, P. Vandamme, J. Walter, K. Watanabe, S. Wuyts, G.E. Felis, M. G. Gänzle, S. Lebeer, A taxonomic note on the genus *Lactobacillus*: description of 23 novel genera, emended description of the genus *Lactobacillus* Beijerinck 1901, and union of *Lactobacillaceae* and *Leuconosto- caceae*, Int. J. Syst. Evol. Micr. 70 (4) (2020) 2782–2858, https://doi.org/10.1099/ijsem.0.004107.

[11] K. Butorac, J. Novak, B. Bellich, L.C. Terán, M. Banić, A. Leboš Pavunc, S. Zjalić, P. Cescutti, J. Šušković, B. Kos, Lyophilized alginate-based microspheres containing *Lactobacillus fermentum* D12, an exopolysaccharides producer, contribute to the strain's functionality *in vitro*, Microb. Cell Fact. 20 (2021) 85, https://doi.org/10.1186/s12934-021-01575-6.

[12] P.T. Nguyen, T.T. Nguyen, D.C. Bui, P.T. Hong, Q.T. Hoang, H.T. Nguyen, Exopolysa- ccharide production by lactic acid bacteria: the manipulation of environmental stresses for industrial applications, AIMS Microbiology 6 (4) (2020) 451, https://doi.org/10.3934/microbiol.2020027.

[13] M.A. Rather, K. Gupta, M. Mandal, Microbial biofilm: formation, architecture, antibiotic resistance, and control strategies, Braz. J. Microbiol. 52 (2021) 1701–1718, https://doi.org/10.1007/s42770-021-00624-x.

[14] Z. Liu, Z. Zhang, L. Qiu, F. Zhang, X. Xu, H. Wei, X. Tao, Characterization and bioactivities of the exopolysaccharide from a probiotic strain of *Lactobacillus plantarum* WLPL04, J. Dairy Sci. 100 (9) (2017) 6895–6905, https://doi.org/10.3168/jds.2016-11944.

[15] M.L. Werning, A.M. Hernández-Alcántara, M.J. Ruiz, L.P. Soto, M.T. Dueñas, P. López, L.S. Frizzo, Biological functions of exopolysaccharides from lactic acid bacteria and their potential benefits for humans and farmed animals, Foods 11 (9) (2022) 1284, https://doi.org/10.3390/foods11091284.

[16] M. Živković, M.S. Miljković, P. Ruas-Madiedo, M.B. Markelić, K. Veljović, M. Tolinački, S. Soković, A. Korać, N. Golić, EPS-SJ exopolisaccharide produced by the strain *Lactobacillus paracasei* subsp. *paracasei* BGSJ2–8 is involved in adhesion to epithelial intestinal cells and decrease on *E. coli* association to Caco-2 cells, Front. Microbiol. 7 (2016) 286, https://doi.org/10.3389/fmicb.2016.00286.

[17] M. Banić, K. Butorac, N. Čuljak, A. Leboš Pavunc, J. Novak, B. Bellich, S. Kazazić, S. Kazazić, P. Cescutti, J. Šušković, J. Zucko, B. Kos, The Human Milk Microbiota Produces Potential Therapeutic Biomolecules and Shapes the Intestinal Microbiota of Infants, Int. J. Mol. Sci. 23 (22) (2022) 14382, https://doi.org/10.3390/ijms232214382.

[18] E.C. Ale, M.F. Rojas, J.A. Reinheimer, A.G. Binetti, *Lactobacillus fermentum*: could EPS production ability be responsible for functional properties? Food Microbiol. 90 (2020) 103465 https://doi.org/10.1016/j.fm.2020.103465.

[19] C.Y. Boquien, Human milk: an ideal food for nutrition of preterm newborn, Front. Pediatr. 6 (2018) 295, https://doi.org/10.3389/fped.2018.00295.

[20] L. Zhang, B. Zhao, C.J. Liu, E. Yang, Optimization of biosynthesis conditions for the production of exopolysaccharides by *Lactobacillus plantarum* SP8 and the exopolysaccharides antioxidant activity test, Indian J. Microbiol. 60 (2) (2020) 334–345, https://doi.org/10.1007/s12088-020-00865-8.

[21] N. Castro-Bravo, J.M. Wells, A. Margolles, P. Ruas-Madiedo, Interactions of surface exopolysaccharides from *Bifidobacterium* and *Lactobacillus* within the intestinal environment, Front. Microbiol. 9 (2018) 2426, https://doi.org/10.3389/fmicb.2018.02426.

[22] M. Banić, K. Uroić, A. Leboš Pavunc, J. Novak, K. Zorić, K. Durgo, H. Petković, P. Jamnik, S. Kazazić, S. Kazazić, S. Radović, S. Scalabrin, U. Hynönen, J. Šušković, B. Kos, Characterization of S-layer proteins of potential probiotic starter culture *Lactobacillus brevis* SF9B isolated from sauerkraut, LWT–Food Sci. Technol. 93 (2018) 257–267, https://doi.org/10.1016/j. lwt.2018.03.054.

[23] R.K. Aziz, D. Bartels, A.A. Best, M. DeJongh, T. Disz, R.A. Edwards, K. Formsma, S. Gerdes, E.M. Glass, M. Kubal, F. Meyer, G.J. Olsen, R. Olson, A.L. Osterman, R. A. Overbeek, L.K. McNeil, D. Paarmann, T. Paczian, B. Parrello, G.D. Pusch, C. Reich, R. Stevens, O. Vassieva, V. Vonstein, A. Wilke, O. Zagnitko, The RAST server: rapid annotations using subsystems technology, BMC Genomics 9 (1) (2008) 1–15, https://doi.org/10.1186/1471-2164-9-75.

[24] N.F. Alikhan, N.K. Petty, N.L. Ben Zakour, S.A. Beatson, BLAST Ring Image Generator (BRIG): simple prokaryote genome comparisons, BMC genomics 12 (1) (2011) 1–10. doi:10. 1186/1471–2164–12-402.

[25] A.J. van Heel, A. de Jong, C. Song, J.H. Viel, J. Kok, O.P. Kuipers, BAGEL4: a user-friendly web server to thoroughly mine RiPPs and bacteriocins, Nucleic Acids Res. 46 (W1) (2018) W278–W281, https://doi.org/10.1093/nar/gky383.

[26] R. Tallon, P. Bressollier, M.C. Urdaci, Isolation and characterization of two exopolysa- ccharides produced by *Lactobacillus plantarum* EP56, Res. Microbiol. 154 (10) (2003) 705–712, https://doi.org/10.1016/j.resmic.2003.09.006.

[27] K. Wang, W. Li, X. Rui, X. Chen, M. Jiang, M. Dong, Characterization of a novel exopolysaccharide with antitumor activity from *Lactobacillus plantarum* 70810, Int. J. Biol. Macromol. 63 (2014) 133–139, https://doi.org/10.1016/j.ijbiomac.2013.10.036.

[28] B. Bellich, N. Janež, M. Sterniša, A. Klančnik, N. Ravenscroft, R. Rizzo, J. Sabotič, P. Cescutti, Characterisation of a new cell wall teichoic acid produced by *Listeria innocua* ŽM39 and analysis of its biosynthesis genes, Carbohydr. Res. 511 (2022) 108499, https://doi.org/10.1016/j. carres.2021.108499.

[29] S. Manna, J.P. Werren, B.D. Ortika, B. Bellich, C.L. Pell, E. Nikolaou, I. Gjuroski, S. Lo, J. Hinds, O. Tundev, E.M. Dunne, B.D. Gessner, S.D. Bentley, F.M. Russell, E. K. Mulholland, T. Mungun, C. von Mollendorf, P.V. Licciardi, P. Cescutti, N. Ravenscroft, M. Hilty, C. Satzke, *Streptococcus pneumoniae* serotype 33G: genetic, serological, and structural analysis of a new capsule type, Microbiology spectrum 12 (1) (2024), https://doi.org/10.1128/spectrum.03579-23 e03579–23.

[30] D.P. Sweet, R.H. Shapiro, P. Albersheim, Quantitative analysis by various g.l.c. response-factor theories for partially methylated and partially ethylated alditol acetates, Carbohydr. Res. 40 (1975) 217–225, https://doi.org/10.1016/S0008-6215(00)82604-X.

[31] G.J. Gerwig, J.P. Kamerling, J.F.G. Vliegenthart, Determination of the D and L configuration of neutral monosaccharides by high-resolution capillary GLC, Carbohydr. Res. 62 (1978) 349–357, https://doi.org/10.1016/S0008-6215(00)80881-2.

[32] B. Bellich, I.A. Jou, C. Buriola, N. Ravenscroft, J.W. Brady, M. Fazli, T. Tolker-Nielsen, R. Rizzo, P. Cescutti, The biofilm of *Burkholderia cenocepacia* H111 contains an exopolysaccharide composed of L-rhamnose and L-mannose: structural characterization and molecular modelling, Carbohydr. Res. 499 (2021) 108231, https://doi.org/10.1016/j.carres.2020.108231.

[33] K. Butorac, M. Banić, J. Novak, A. Leboš Pavunc, K. Uroić, K. Durgo, N. Oršolić, M. Kukolj, S. Radović, S. Scalabrin, J. Žučko, A. Starčević, J. Šušković, B. Kos, The functional capacity of plantaricin-producing *Lactobacillus plantarum* SF9C and S-layer-carrying *Lactobacillus brevis* SF9B to withstand gastrointestinal transit, Microb. Cell Fact. 19 (2020) 1–16, https://doi.org/10.1186/s12934-020-01365-6.
[34] Statistics Kingdom, One-way ANOVA Calculator and Tukey HSD, Statistics Kingdom: Website for Statistics calculators, Melbourne, Australia; 2017, Available from: http://www.statskingdom.com, 2017.
[35] W. Zhang, H. Zhang, Genomics of lactic acid Bacteria, in: H. Zhang, Y. Cai (Eds.), Lactic Acid Bacteria, Springer, Dordrecht, 2014, pp. 205–247.
[36] M. Verce, L. De Vuyst, S. Weckx, Comparative genomics of *Lactobacillus fermentum* suggests a free-living lifestyle of this lactic acid bacterial species, Food Microbiol. 89 (2020) 103448, https://doi.org/10.1016/j.fm.2020.103448.
[37] B.K. Mishra, S. Das, S.K. Nandy, M. Patel, S. Hati, Genomic and probiotic attributes of *Lactobacillus* strains from rice-based fermented foods of north eastern India, J. Food Sci. Tech. 60 (2) (2023) 504–516, https://doi.org/10.1007/s13197-022-05633-8.
[38] A.A. Zeidan, V.K. Poulsen, T. Janzen, P. Buldo, P.M. Derkx, G. Øregaard, A. R. Neves, Polysaccharide production by lactic acid bacteria: from genes to industrial applications, FEMS microbial. Rev. 41 (Supp_1) (2017) S168–S200.
[39] Y. Zhou, Y. Cui, X. Qu, Exopolysaccharides of lactic acid bacteria: structure, bioactivity and associations: a review, Carbohydr. Polym. 207 (2019) 317–332, https://doi.org/10.1016/j.carbpol.2018. 11.093.
[40] P.E. Jansson, L. Kenne, G. Widmalm, Computer-assisted structural analysis of polysaccha- rides with an extended version of CASPER using 1H-and 13C-NMR data, Carbohydr. Res. 188 (1989) 169–191, https://doi.org/10.1016/0008-6215(89)84069-8.
[41] R.R. Kapaev, K.S. Egorova, P.V. Toukach, Carbohydrate structure generalization scheme for database-driven simulation of experimental observables, such as NMR chemical shifts, J. Chem. Inf. Model. 54 (9) (2014) 2594–2611, https://doi.org/10.1021/ci500267u.
[42] R.R. Kapaev, P.V. Toukach, Improved carbohydrate structure generalization scheme for 1H and 13C NMR simulations, Anal. Chem. 87 (14) (2015) 7006–7010, https://doi.org/10.1021/acs.analchem. 5b01413.
[43] P.V. Toukach, K.S. Egorova, Carbohydrate structure database merged from bacterial, archaeal, plant and fungal parts, Nucleic Acids Res. 44 (D1) (2016) D1229–D1236, https://doi.org/10.1093/nar/gkv840.
[44] R.R. Kapaev, P.V. Toukach, GRASS: semi-automated NMR-based structure elucidation of saccharides, Bioinformatics 34 (6) (2018) 957–963, https://doi.org/10.1093/bioinformatics/btx696.
[45] P.V. Toukach, V.P. Ananikov, Recent advances in computational predictions of NMR parameters for structure elucidation of carbohydrates: methods and limitations, Chem. Soc. Rev. 42 (2013) 8376–8415, https://doi.org/10.1039/C3CS60073D.
[46] A. Monteagudo-Mera, R.A. Rastall, G.R. Gibson, D. Charalampopoulos, A. Chatzifragkou, Adhesion mechanisms mediated by probiotics and prebiotics and their potential impact on human health, Appl. Microbiol. Biot. 103 (2019) 6463–6472, https://doi.org/10.1007/s00253-019-09978-7.
[47] N. Čuljak, A. Leboš Pavunc, K. Dučkić, K. Butorac, M. Banić, J. Novak, J. Šušković, B. Kos, Functionality and protective effect of S-layer proteins in microencapsulated freeze-dried probiotic *Levilactobacillus brevis* strains, Mljekarstvo 74 (3) (2024) (in press).
[48] J. Šušković, B. Kos, J. Beganović, A. Leboš Pavunc, K. Habjanič, S. Matošić, Antimicrobial activity–the most important property of probiotic and starter lactic acid bacteria, Food Technol. Biotech. 48 (3) (2010) 296–307. https://hrcak.srce.hr/57561.
[49] C.M.A.P. Franz, M.J. Van Belkum, W.H. Holzapfel, H. Abriouel, A. Gálvez, Diversity of enterococcal bacteriocins and their grouping in a new classification scheme, FEMS Microbiology Reviews 31 (3) (2007) 293–310, https://doi.org/10.1111/j.1574-6976.2007.00064.x.
[50] C.I. dos Santos, C.D.L. Campos, W.R. Nunes-Neto, M.S. do Carmo, F.A.B. Nogueira, R.M. Ferreira, E.P.S. Costa, L.F. Gonzaga, J.M.M. Araújo, J.M. Monteiro, C.R.A. V. Monteiro, F.S. Planter, I.F.S. Figueiredo, R.A. Holanda, S.G. Monteiro, E. S. Fernandes, A.S. Monteiro, V. Monteiro-Neto, Genomic Analysis of *Limosilactobacillus fermentum* ATCC 23271, a Potential Probiotic Strain with Anti-Candida Activity, J. Fungi 7 (10) (2021) 794, https://doi.org/10.3390/jof7100794.
[51] I. Falasconi, A. Fontana, V. Patrone, A. Rebecchi, G. Duserm Garrido, L. Principato, M.L. Callegari, G. Spigno, L. Morelli, Genome-assisted characterization of *Lactobacillus fermentum*, *Weissella cibaria*, and *Weissella confusa* strains isolated from sorghum as starters for sourdough fermentation, Microorganisms 8 (9) (2020) 1388, https://doi.org/10.3390/microorganisms8091388.
[52] J. Novak, K. Butorac, A. Leboš Pavunc, M. Banić, A. Butorac, A. Lepur, N. Oršolić, K. Tonković, K. Bendelja, N. Čuljak, M. Lovrić, J. Šušković, B. Kos, A lactic acid Bacteria consortium impacted the content of casein-derived biopeptides in dried fresh cheese, Molecules 27 (1) (2021) 160, https://doi.org/10.3390/molecules27010160.
[53] H.I. Ahmed, E. Ransom-Jones, S. Sadiq, A. Vitlic, N. McLay, M.F. Rojas, E.C. Ale, A. G. Binetti, A. Collett, P.N. Humphreys, A.P. Laws, Structural characterisation of two medium molecular mass exopolysaccharides produced by the bacterium *Lactobacillus fermentum* Lf2, Carbohydr. Res. 488 (2020) 107909, https://doi.org/10.1016/j.carres.2020.107909.